Formation of Group 11 Metal(I)-Arene Complexes: Bonding Mode and Molecule-Responsive Spectral Variations

Feng-Bo Xu,[†] Qing-Shan Li,[†] Li-Zhu Wu,[‡] Xue-Bing Leng,[†] Zu-Cheng Li,[†] Xian-Shun Zeng,[†] Yuan L. Chow,[§,†] and Zheng-Zhi Zhang*[,†]

State Key Laboratory of Elemento-Organic Chemistry, Nankai University, Tianjin 300071, People's Republic of China, and Technical Institute of Physics and Chemistry, the Chinese Academy of Sciences, Beijing 100101, People's Republic of China

Received August 15, 2002

Two N(*n*-Pr)PPh_2 groups appended to the 9,10-anthracene positions through methylene spacers as a bidentate ligand coordinate with Cu^+, Ag^+, and Au^+ ions efficiently to afford *endocyclic* metal complexes with metal-η^6-arene bonding, rarely observed for the group 11 metal ions. The three-center metal−NP and metal−η^6-arene bonding patterns in the *endocyclic* complexes were confirmed using ab initio and density functional calculations. The close metal−anthracene centroid distances significantly affected absorption and fluorescence properties of the complexes in solution. Among them the Cu^+ complex has the shortest metal−anthracene distance and most drastic spectral abnormality. The close distances also controlled the *endocyclic-exocyclic* metal transition of the complexes, wherein the equilibrium heavily favored the former on account of η^6 interactions. These complexes reacted with phosphines in solution to give highly fluorescent species that were proposed to possess the *exocyclic* configuration with the three-coordinated metal center. These *exocyclic* metal complexes as well as the ligand itself all form respective excimers from their singlet excited states to exhibit an additional broad fluorescence at about 455 nm. The excimers are assumed to arise from an interaction of the excited anthracene moiety with an N−P group of the ground state *exocyclic* molecule. The observed molecule-responsive light-switchable spectral variations have been discussed in terms of structural changes in the *endocyclic-exocyclic* metal transitions.

Introduction

Studies of fluoroionophores have attracted much attention in the past decade[1−3] owing to their enormous potential for application as molecular sensors in many fields related to life and living. Fluoroionophore sensors generally consist of an ion-binding component transduced to a signaling unit; the latter generally uses fluorescence variations as indicators,[1a,b] which have distinct advantages in terms of sensitivity, selectivity, and response time. As binding components, chelators, podands, coronands, and cryptands[1b] containing a number of heteroatoms of group 15 and 16 elements are commonly used. Characteristically, these ionophore components are designed with a finite cavity size for selectivity purposes and are constructed around or attached to a fluorophore component,[1f] for which anthracene has many advantages (such as its strong fluorescent behavior and ease of functionalization) and has been used widely.[2,3] Many studies have revealed a variety of recognition mechanisms on binding and photophysical events.[1e,f]

Ligands with the nitrogen−phosphorus bond contribute to an important group of compounds.[4,5] Whereas both elements are extensively used as coordinating heteroatoms in ionophore designs, a N−P group as a composite center for coordination has seldom been tested, which has prompted us to explore its application in fluoroionophore chemistry. Our design is that each N(*n*-Pr)PPh_2 group through one methylene spacer was attached to the 9,10-positions of anthracene, as shown

* Corresponding author. E-mail: zzzhang@public.tpt.tj.cn.
[†] State Key Laboratory of Elemento-Organic Chemistry, Nankai University.
[‡] Technical Institute of Physics and Chemistry, the Chinese Academy of Sciences.
[§] Emeritus Professor at Simon Fraser University, Burnaby, Canada.

(1) (a) Czarnik, A. W. In *Topics in Fluorescence Spectroscopy*; Rakowicz, J., Ed.; Plenum Press: New York, 1994; Vol. 4, p 49. (b) Valeur, B. In *Topics in Fluorescence Spectroscopy*; Rakowicz, J., Ed.; Plenum Press: New York, 1994; Vol. 4, p 21. (c) Bissell, R. A.; de Silva, A. P.; Gunaratne, H. Q. N.; Lynch, P. L. M.; Maguire, G. E. M.; McCoy, C. P.; Sandanayake, K. R. A. S. *Top. Curr. Chem.* **1993**, *168*, 223. (d) Czarnik, A. W. *Acc. Chem. Res.* **1994**, *27*, 302. (e) Fabbrizzi, L.; Poggi, A. *Chem. Soc. Rev.* **1995**, 197. (f) de Silva, A. P.; Gunaratne, H. Q. N.; Gunnlangsson, T.; Huxley, A. J. M.; McCoy, C. P.; Rademacher, J. T.; Rice, T. E. *Chem. Rev.* **1997**, *97*, 1515.

(2) (a) Fages, F.; Desvergne, J. P.; Bouas-Laurent, H.; Marsau, P.; Lehn, J. M.; Kotzyba-Hibert, F.; Albrecht-Gary, A. M.; Al-Joubbeh, M. *J. Am. Chem. Soc.* **1989**, *111*, 8672. (b) Desvergne, J. P.; Fages, F.; Bouas-Laurent, H.; Marsau, P. *Pure Appl. Chem.* **1992**, *62*, 1231. (c) Ishikawa, J.; Sakamoto, H.; Nakao, S.; Wada, H. *J. Org. Chem.* **1999**, *64*, 1913.

(3) (a) Fages, F.; Desvergne, J. P.; Bouas-Laurent, H. *J. Am. Chem. Soc.* **1989**, *111*, 96. (b) We are grateful to Professor J. P. Desvergne for making the fluorescence excitation and absorption spectra of 9,10-dipropylanthracene available to us.

(4) Cotton, F. A.; Wilkinson, G. *Advanced Inorganic Chemistry*; John Wiley: New York, 1980; p 460.

(5) (a) Riess, J. G. *Phosphorus Sulfur* **1986**, *27*, 93. (b) Shaw, R. A. *Pure Appl. Chem.* **1975**, *44*, 317. (c) Krishnamurthy, S. S. *Phosphorus, Sulfur Silicon* **1994**, *87*, 101.

10.1021/om020668h CCC: $25.00
Publication on Web 01/11/2003

Scheme 1

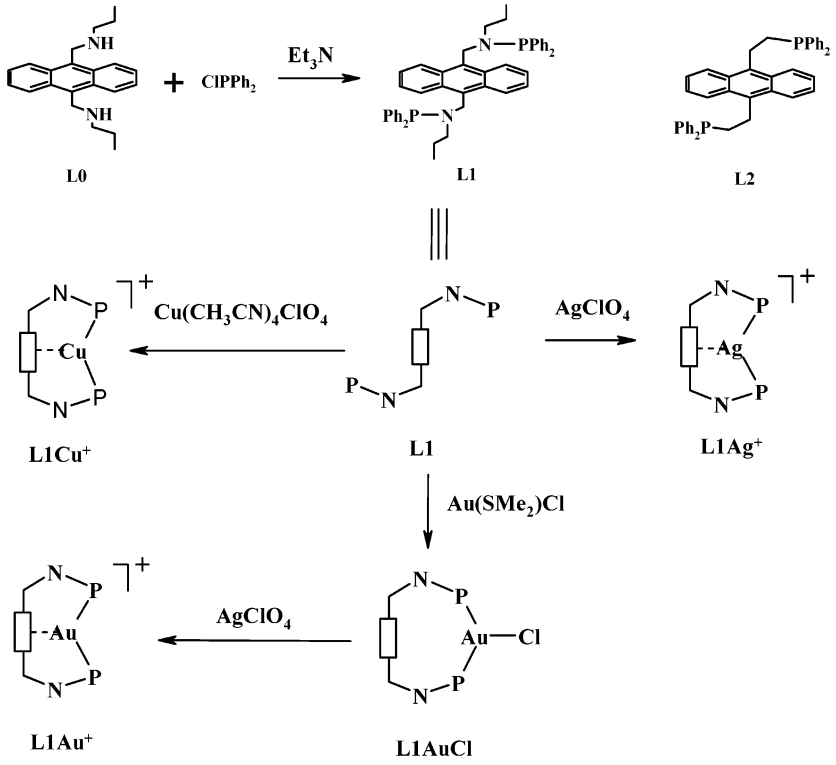

Scheme 2

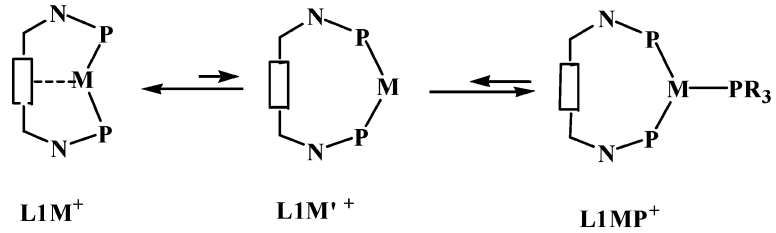

in 9,10-bis{*N*-*n*-propyl-*N*-(diphenylphosphino)aminomethyl}anthracene (L1), which has been prepared for the study (Scheme 1). We wish to describe L1 in the formation of group 11 metal complexes and unusual chemistry thereof. For comparison, 9,10-bis{(2-diphenylphosphino)ethyl}anthracene (L2) is also prepared and its reaction with $AgClO_4$ is studied.

Results and Discussion

Ligands and Metal Complexes. The ligand L1 was synthesized from 9,10-bis(*N*-propylaminomethyl)anthracene (L0)[6] and chlorodiphenylphosphine in the presence of triethylamine to scavenge hydrogen chloride in anhydrous benzene under a nitrogen atmosphere.[10a] L0 was readily prepared from 9,10-bis(chloromethyl)anthracene and *n*-propylamine.[7] L1 in dichloromethane under nitrogen was reacted with silver(I) perchlorate to give L1-silver(I) (abbreviated as $L1Ag^+$) perchlorate in good yield.[10a] Under similar conditions L1 reacted with $Cu(CH_3CN)_4ClO_4$ to afford L1-copper(I) ($L1Cu^+$) perchlorate. L1 reacted with $Au(Me_2S)Cl$ to afford L1-gold(I) chloride (L1AuCl), which was converted to L1-gold(I) ($L1Au^+$) perchlorate by treating with silver perchlorate in dichloromethane. $L1Au^+$ was also obtained by a sequential reaction of L1 with the two reagents in a one-pot operation. These chelated complexes with η^6 bonding[8,9] to the central ring of the anthracene (see Scheme 1) have been confirmed by X-ray analysis; the cycle coordinated with metal by η^6 bonding is referred to as *endocyclic* metal coordination. L1AuCl obviously possessed a covalent Au−Cl bond without η^6 bonding with the anthracene ring and has a structure with a full cycle that is referred to as *exocyclic* metal coordination (also see Scheme 2). A brief account on the preparation and properties of $L1Ag^+$ was published previously.[10a] All these L1-metals were stable in crystalline states for extended storage and also in solution for several weeks. The ligand L2 was prepared from 9,10-bis(2-chloroethyl)anthracene with Ph_2PLi and reacted with $AgClO_4$ under similar conditions to give L2-silver ($L2Ag^+$) perchlorate (Scheme 1).

The ORTEP view of $L1Cu^+$ is shown in Figure 1 as a representative example: $L1Au^+$ in Supporting Informa-

(6) (a) Hong, S. Y.; Czarnik, A. W. *J. Am. Chem. Soc*, **1993**, *115*, 3330. (b) Akkaya, E. U.; Huston, M. E.; Czarnik, A. W. *J. Am. Chem. Soc.* **1990**, *112*, 3590.

(7) Badger, G. M.; Cook, J. W. *J. Chem. Soc.* **1939**, 802.

(8) Mascal, M.; Kerdelhué, J. L.; Blake, A. J.; Cooke, P. A. *Angew. Chem., Int. Ed.* **1999**, *38*, 1968.

(9) Andrianatoandro, H.; Bararns, Y.; Marsau, P.; Desbergne, J. P.; Fages, F.; Bouas-Laurent, H. *Acta Crystallogr.* **1995**, *B51*, 293.

(10) (a) Xu, F. B.; Weng, L. H.; Sun, L. J.; Zhang, Z. Z. *Organometallics* **2000**, *19*, 2658. (b) Xu, F. B. Ph.D. Dissertation, Institute of Elemento-Organic Chemistry, Nankai University, June 2001.

Table 1. Selected Bond Distances, Bond Angles, and Related Data of the Ligand and Complexes

compond	L1	$L1CuClO_4$	$L1AgClO_4$	$L1AuClO_4$	$L2AgClO_4$
P(1)−N(1) (Å)	1.664	1.666	1.669	1.672	
P(2)−N(2) (Å)	1.680	1.657	1.671	1.664	
P(1)-M(I) (Å)		2.136	2.4029	2.3208	2.439
P(2)−M(I) (Å)		2.2140	2.4056	2.3239	2.440
P(1)−M(I)−P(2) (deg)		153.97	169.9	171.6	177.9
C(1)−C(2)−C(9) (deg)	175.9	169.6	172.4	169.0	171.2
C(2)−C(9)−C(16) (deg)	175.9	168.5	171.5	171.1	168.5
M(I)−An (Å)[a]		2.498	2.79	3.00	3.148
M(I)−C_{an} (Å)[b]		2.773−3.021	3.053−3.157	3.118−3.246	3.282−3.606
angle of An (deg)[c]	180	172.3	175.4	176.1	174.7
An−An (Å)[d]		5.075	4.336	4.312	
An+An (Å)[e]		3.5896	3.4162	3.4076	

[a] The distance of the metal ion to the centroid of anthracene. [b] The distances of the metal ion to the six carbon atoms of the middle ring in anthracene. [c] The dihedral angle between the two side rings in anthracene. [d] The distance between the two centroids of the two $\pi-\pi$ stacking anthracene rings. [e] The distance between the two planes of the two $\pi-\pi$ stacking anthracene rings.

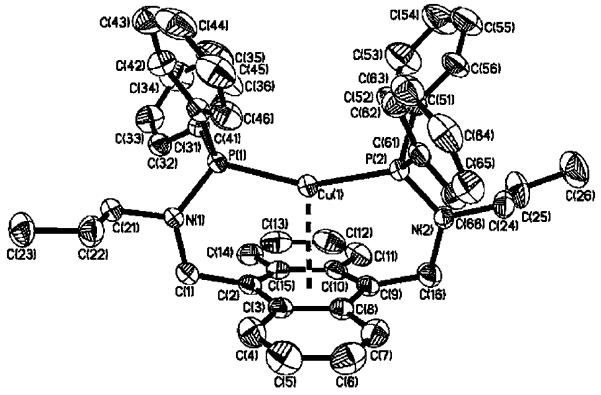

Figure 1. ORTEP view of $L1Cu^+$.

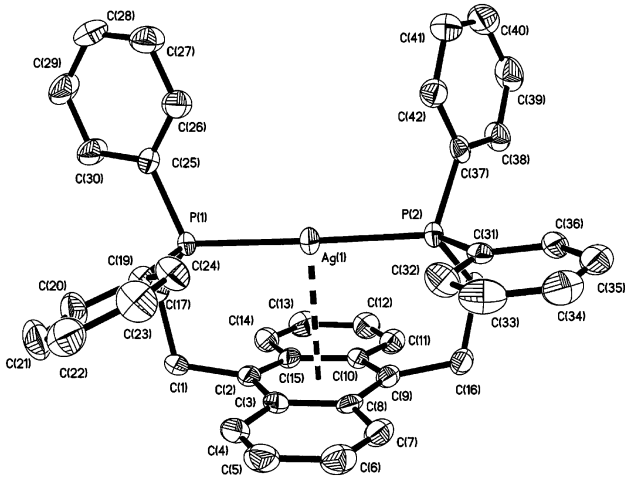

Figure 2. ORTEP view of $L2Ag^+$.

tion and $L1Ag^+$ in ref 10a. For comparison, the crystal structure of $L2Ag^+$ is shown in Figure 2. Some molecular dimensions characteristic of these metal complexes and pertinent for the discussion are listed in Table 1. The first significant feature was the bonding of the metal to six carbon atoms of the anthracene central ring, indicating a η^6 coordination mode; that is, the distance of the metal to the centroid of the mid-benzene ring was short, and that in $L1Cu^+$ (at 2.498 Å) was distinctly shorter than the corresponding distance in the other two. Second, two anthracene 9,10-carbon atoms were markedly bent forward out of coplanar configuration. Also, the two side benzene rings were bent backward at the anthracene 9,10-carbons probably through rehybridization to a nonplanar configuration (i.e., with a higher order than sp^2); the dihedral angle between the two side rings in $L1Cu^+$ was the smallest (at 172.3°) in comparison to that in the other two. Third, the anthracene rings were closely packed in parallel at about 3.41 Å distance for $L1Ag^+$ and $L1Au^+$; for $L1Cu^+$ the $\pi-\pi$ stacking was staggered and the corresponding distance is 3.59 Å. These features are rare phenomena for group 11 metal ions. There is only one example of η^6-π bonding for Cu^+,[8] two for Ag^+,[8,9] and none for Au^+. The metal−arene centroid distance at 2.50 Å for $L1Cu^+$ and 2.79 Å for $L1Ag^+$ are the shortest ever observed among all known examples; the closest reported values prior to this report were 2.97 Å[8] and 2.92 Å,[9] respectively. However, the Ag−anthracene centroid distance is 3.148 Å in the *endocyclic* coordination $L2Ag^+$ (Scheme 2). L2 reacts with the other reagents $Cu(CH_3CN)_4ClO_4$ and $Au(SMe_2)Cl$, respectively, to give complexes with completely different structures.[10b]

Ligand L1, as a bidentate coordinating unit, can easily clutch these univalent group 11 metal ions; that capacity should be credited to its two N−P functions to chelate the metals over the space above the anthracene π-face.

The bonding features in these *endocyclic* complexes ($L1Cu^+$, $L1Ag^+$, and $L2Ag^+$) were also examined using both ab initio (Hartree−Fock, HF) and density functional (hybrid nonlocal, B3LYP) methods.[11a] The results (Table 2) from Bader's atoms-in-molecule (AIM) analysis of the electron densities[11e] are emphasized, although all relevant molecular orbitals (MOs from HF/LanL2DZ) and Kohn−Sham orbitals (KSOs from B3LYP/LanL2DZ) have also been examined carefully. According to Bader's AIM theory,[11e] there is bonding if a bond critical point (BCP) is found around the connecting line between the two atoms, or among three or more atoms. Furthermore, for similar bonds, the larger the electron density (ρ) at the BCP, the stronger the bond is. Table 2 presents the values of electron density ρ, ellipticity ($\epsilon = \lambda_1/\lambda_2 - 1$),

(11) (a) Frisch, M. J.; Trucks, G. W.; Schlegel, H. B.; et al. *Gaussian 98* (Revision A.7); Gaussian, Inc.: Pittsburgh, PA, 1998. (b) For example: Petersson, G. A.; Bennett, A.; Tensfeldt, T. G.; Al-Laham, M. A.; Shirley, W. A.; Mantzaris, J. *J. Chem. Phys.* **1988**, *89*, 2193. (c) Curtiss, L. A.; McGrath, M. P.; Blaudeau, J.-P.; Davis, N. E.; Binning, R. C., Jr.; Radom, L. *J. Chem. Phys.* **1995**, *103*, 6104. (d) For example: Kaupp, M.; Schleyer, P. V. R.; Stoll, H.; Preuss, H. *J. Chem. Phys.* **1991**, *94*, 1360, and references therein. (e) Bader, R. F. W *Atoms in Molecules*: *A Quantum Theory*; Oxford University Press: Oxford, 1990. (f) Note: these results are similar to those calculated from B3LYP/3-21G*. For example, for L1Ag, B3LYP/3-21G* gave BCP electron densities of 0.078, 0.165, 0.016 e/a_0^3 for Ag−P, N−P, and Ag−C_{ring} bonds, respectively, and other properties are also similar. (g) The plots were made using: Schaftenaar, G. *Molden*; CAOS/CAMM Center Nijmegen: Toernooiveld, Nijmegen, The Netherlands, 1991.

Table 2. B3LYP/STO-3G* AIM Bonding Properties (in atomic units, i.e., ρ in e/a_0^3 and $\nabla^2\rho$ in e/a_0^5) of Complexes L1Cu$^+$, L1Ag$^+$, and L2Ag$^+$

molecule	bond[a]	ρ	$\nabla^2\rho$	ϵ	λ_1	λ_2	λ_3
L1Cu$^+$	Cu−P	0.098	0.122	0.040	−0.079	−0.076	0.277
L1Ag$^+$	Ag−P	0.081	0.187	0.021	−0.080	−0.078	0.344
L2Ag$^+$	Ag−P	0.069	0.150	0.005	−0.066	−0.065	0.281
L1Cu$^+$	N−P	0.158	0.780	0.227	−0.219	−0.178	1.178
L1Ag$^+$	N−P	0.157	0.742	0.213	−0.214	−0.177	1.130
L2Ag$^+$	C−P	0.149	−0.079	0.110	−0.169	−0.152	0.242
L1Cu$^+$	Cu−C_{ring}	0.021	0.066	5.511	−0.015	−0.002	0.083
L1Ag$^+$	Ag−C_{ring}	0.012	0.046	1.126	−0.006	−0.003	0.054
L2Ag$^+$	Ag−C_{ring}	0.007	0.023	4.504	−0.004	−0.001	0.028

[a] M−C_{ring} denotes the metal atom weakly bonding with a carbon atom in the central phenyl ring detected in the AIM analysis, and each M−C_{ring} stands for two slightly different bonds except for L2Ag$^+$, which has only one such bond found, and so the data for each bond are an arithmetic average except for L2Ag$^+$.

and other properties at the BCPs of the relevant bonds in these complexes obtained using B3LYP/STO-3G*[11f]

As shown in Table 2, the most important feature is that the bonding in L1Cu$^+$ is overall much stronger than that in L1Ag$^+$, which is, in turn, much stronger than L2Ag$^+$. First, the Cu−P bond possesses larger electron density than the Ag−P bond (0.098 vs 0.081 e/a_0^3), indicating the different bond strength. Second, the bonding between the metal and N−P group in L1Cu$^+$ is modestly stronger than that in L1Ag$^+$, as indicated by its larger ellipticity (ϵ), implying its slightly greater orbital overlap in the Cu−NP triangle than in the Ag−NP one (Figure 3). Third, the electron densities on the Cu−C_{ring} bonds (C_{ring} denotes a C atom in the central ring of the anthracene) are much denser than those on corresponding Ag−C_{ring} bonds in L1Ag$^+$ (0.021 vs 0.012 e/a_0^3), demonstrating that the former are stronger than the latter. This indicates that Cu−η^6-arene bonding in L1Cu$^+$ must be stronger than Ag−η^6-arene in L1Ag$^+$ because a M−C_{ring} bond represents a localized metal−η^6-arene coordination. These results also agree well with crystal structure features of these complexes.

The comparison of the bonding data of L1Ag$^+$ with respect to those of L2Ag$^+$ provides the important contribution of the N−P group to the complex formation. First, the electron density on the Ag−P bond in L1Ag$^+$ is larger than that in L2Ag$^+$. Second, although the average Ag−N distance is around 3.5 Å, which indicates no direct bond is formed between them, the far larger ellipticity of the N−P bond in L1Ag$^+$ than that of the C−P bond in L2Ag$^+$ (0.213 vs 0.110 e/a_0^3) indicates that the former would favor the formation of the three-center Ag−NP bonding much more significantly over the Ag−CP bonding. In fact, inspection of relevant MOs for these two complexes reveals that the Ag−NP bonding is present, whereas the Ag−CP cannot be found (see Figure 3[11g]). Third, as represented by the Ag−C_{ring} bonds, the Ag−η^6-arene bond in L1Ag$^+$ is also much stronger than that in L2Ag$^+$. These theoretical results clearly indicate that there are three-center, triangle metal−NP bonding and metal−η^6-arene coordinating features shown in the crystal structures for these *endocyclic* complexes L1M$^+$.

In studies of absorption, fluorescence and excitation spectra of L1 and L1M 9,10-diisopropylanthracene[3] and anthracene itself were used as the reference. The absorption spectra (Figure 4a) showed that L1Ag$^+$ and L1Au$^+$ possessed the L1 type absorption pattern (essentially an anthracene type)[2,3] with red-shifts. In contrast, L1Cu$^+$ showed a broad charge transfer band visibly different from that of the other two. The broad absorption spectrum of L1Cu$^+$ is probably a consequence of the shorter Cu−anthracene centroid distance and the bending of the two side benzene rings out of coplanarity (Table 1) and suggests that the original rigid anthracene configuration is destroyed. The absorption spectrum is obviously dominated by a ligand-to-metal charge transfer process. L1 in dichloromethane showed a strong anthracenoid fluorescence spectrum at $<10^{-6}$ M. As increasing its concentration a broad emission at 455 nm emerged and increased (Figure 5), the corresponding excitation spectra were regular anthracenoid type without such concentration effects. At 10^{-6} M concentration, these L1-metals exhibited weak fluorescence spectra (Figure 4b) that, when enlarged, resembled the pattern of L1 and essentially an anthracenoid type.[2,3] Finally, L1AuCl under comparable conditions showed an intense fluorescence spectrum, as in Figure 6, and also a new broad fluorescence at 456 nm at higher concentrations (at 10^{-4} M).

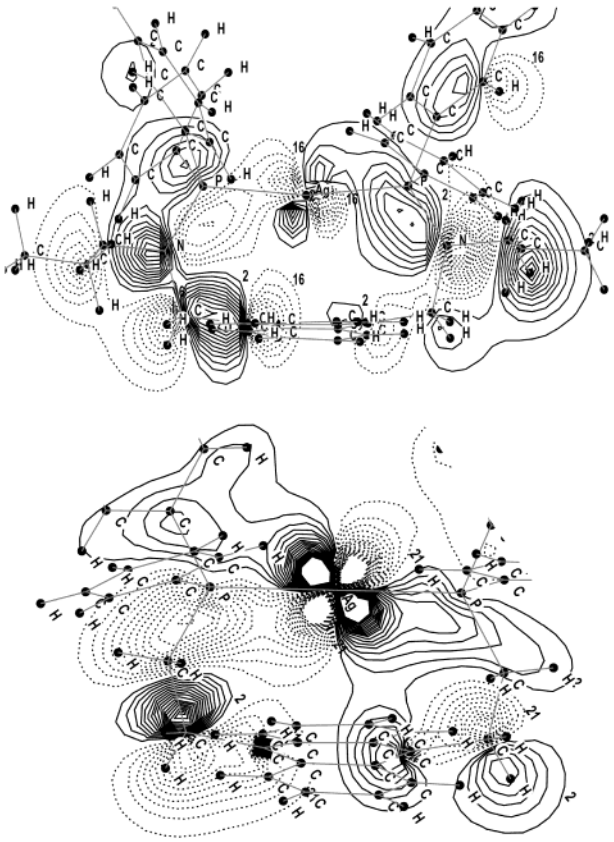

Figure 3. Contour plots of HF/LanL2DZ molecular orbital 159 (upper), which indicates tri-center Ag−CN bonding in L1Ag$^+$, and 117 (lower) in L2Ag$^+$ (for reference) on the plane roughly containing the neighboring N−P−Ag−P−N and C−P−Ag−P−C atoms, respectively. Solid contours are at 0.005, 0.010, ..., 0.095 e/a_0^3, and negative contours are dashed.

The fluorescence decay dynamics of L1 and L1-metal perchlorates were investigated with a single photon counting device to provide lifetimes of their singlet excited state. While L0 and L2 decayed with a clean single exponential to give the lifetimes $\tau = 3.9$ and 2.8 ns, respectively, all L1 and L1-metals did so with double

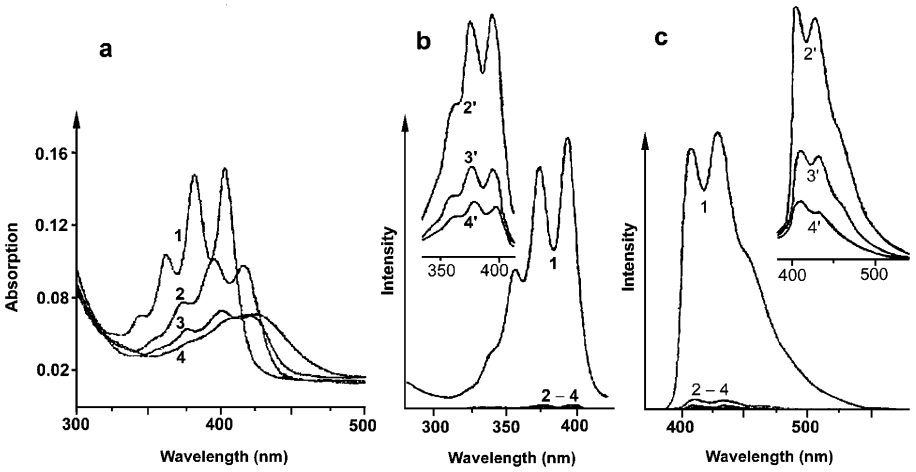

Figure 4. (a) Absorption spectra 1−4 in the order L1, L1Ag$^+$, L1Au$^+$, and L1Cu$^+$ at 1×10^{-6} M in dichloromethane. (b, c) Excitation ($\lambda_{monitor} = 433$ nm) and fluorescence ($\lambda_{ex} = 360$ nm) spectra 1−4 in the order L1, L1Cu$^+$, L1Ag$^+$, and L1Au$^+$ at 5×10^{-6} M in dichloromethane [2′−4′ curves are the amplified spectra of 2−4 in (b and c).

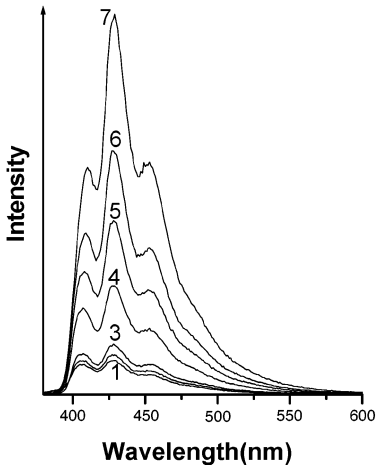

Figure 5. Fluorescence ($\lambda_{ex} = 360$ nm) spectra 1−7 of L1 in order of increasing concentrations at 6×10^{-6}, 8×10^{-6}, 1×10^{-5}, 2×10^{-5}, 4×10^{-5}, 6×10^{-5}, and 1×10^{-4} M in dichloromethane.

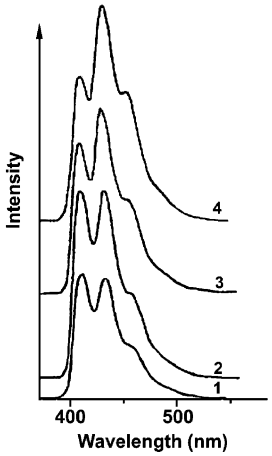

Figure 6. Fluorescence spectra 1−4 of L1AuCl ($\lambda_{ex} = 360$ nm) in order of increasing concentration at 5×10^{-6}, 1×10^{-5}, 5×10^{-5}, and 1×10^{-4} M in dichloromethane.

exponentials to give two lifetimes as shown in Table 3. As the minor component τ_1 (=2−3 ns) increased with the [L1] concentration increase of 10^{-5} to 10^{-4} M and also with the monitoring wavelength 425 nm shifting to 460 nm, this component must be originated from the new broad emission centered at 455 nm caused by higher concentrations (see Figure 5). The major component with $\tau_2 = 9-12$ ns must come from the decay of singlet excited state L1. Therefore, the former minor component was an excimer, formed from dynamic self-quenching of the latter major component (i.e., singlet excited state L1). Though L1-metals have weak fluorescence, both L1Ag$^+$ and L1Cu$^+$ also gave double exponential decay patterns. The quantum yield of fluorescence (Table 3) was determined by using anthracene as the secondary actinometer with $\Phi = 0.27$. The low quantum yields of L1-metals agreed with Figure 4c. It should be mentioned that fluorescence quantum yields were the sum of the two emitting species and must be concentration dependent.

The *endocyclic* structure of L1-metals as defined by X-ray analysis (see Figure 1) is the basis for the discussion of observed spectra in relation to the reaction pattern in Schemes 1 and 2. First of all, weak metal complex fluorescence in Figure 4c is assumed to arise from a lack of L1M$^+$ emission due to the metal−arene interaction, which can be attributed to donation of the anthracene π-electron cloud to the unoccupied 5s orbital of the group 11 metal ion.[12] As L1AuCl shows strong fluorescence spectra in contrast to L1Au$^+$, it must have an *exocyclic* structure similar to that of L1AuP$^+$, as shown in Scheme 1.

The disparity leads us to propose that endocyclic L1M$^+$ and exocyclic L1M′$^+$ are in equilibrium heavily in favor of the former (Scheme 2), which is nonfluorescent, whereas the latter, L1M′$^+$, causes fluorescence in analogy with L1AuCl. It follows that the observed weak emission of the M$^+$ complex solution in Figure 4c arises solely from a low equilibrium concentration of L1M′$^+$.

Interaction of L1-Metal and Phosphines. Whereas the reaction product L1AuP$^+$ of L1-metal perchlorates with diphenylphosphine could not be isolated and only the robust L1-metal perchlorates can be recovered, the solution of L1Au$^+$/PPh_2H (1:5) in $CDCl_3$ revealed four ^{31}P signals at −60 °C (Figure 7). The ^{31}P NMR signals appear at 35.12 and 0.12 ppm for the ring P and

(12) (a) Beberwijk, C. D. M.; van der Kerk, G. J. M.; Leusink, A. J.; Noltas, J. G. *Organomet. Chem. Rev.* **1970**, *45*, 215. (b) Ogimachi, N.; Andrews, L. J.; Keefer, R. M. *J. Am. Chem. Soc.* **1956**, *18*, 2210.

Table 3. Fluorescence Lifetime and Quantum Yield of the Ligand and Complexes in Degassed CH_2Cl_2

	lifetime at 425 nm		lifetime at 460 nm		
compound	τ_1/ns (%)	τ_2/ns (%)	τ_1/ns (%)	τ_2/ns (%)	Φ
L0 (10^{-5}M)	3.9				0.1824
L1(10^{-5} M)	2.7 (7.0)	10.5 (93.0)	3.7 (10.1)	11.8 (89.9)	0.1160
L1 (10^{-4} M)	1.9 (11.5)	8.9 (88.5)	2.2 (15.1)	10.2 (84.9)	
L1CuClO$_4$ (10^{-4} M)	2.3 (19.5)	11.2 (80.5)	0.4 (18.3)	11.6 (81.7)	0.0078
L1AgClO$_4$ (10^{-4} M)	2.4 (22.3)	10.8 (77.4)	0.8 (21.2)	11.1 (78.8)	0.0047
L1AuClO$_4$ (10^{-4} M)					0.0024
L2 (10^{-4}M)			2.8		

external P, respectively, of the complex L1AuP$^+$, in addition to that at 89.13 ppm for L1Au$^+$ and at 25.50 ppm for unreacted PPh_2H. At the L1Au$^+$/PPh_2H ratio of 1:20 in $CDCl_3$ and at −60 °C, the ^{31}P signal of L1Au$^+$ disappeared all together, indicating the complete coordination; at the same time, a signal at −20.17 ppm could be assigned to the external P of the complex L1AuP$^+$, and those at 33.50 and 24.75 ppm to the ring P of L1AuP$^+$ and to bulk PPh_2H, respectively. This solution, on warming up to −20 °C, registered two averaged signals, one at 34.64 ppm for L1AuP$^+$ and the other at 24.14 ppm for Ph_2PH due to a rapid thermal equilibration of coordination between L1M$^+$ and L1MP$^+$. The fact that ^{31}P chemical shift variations depend on both PPh_2H concentration and temperature indicates a dynamic equilibrium of the *endo-exo* cyclic changes as shown in Scheme 2.

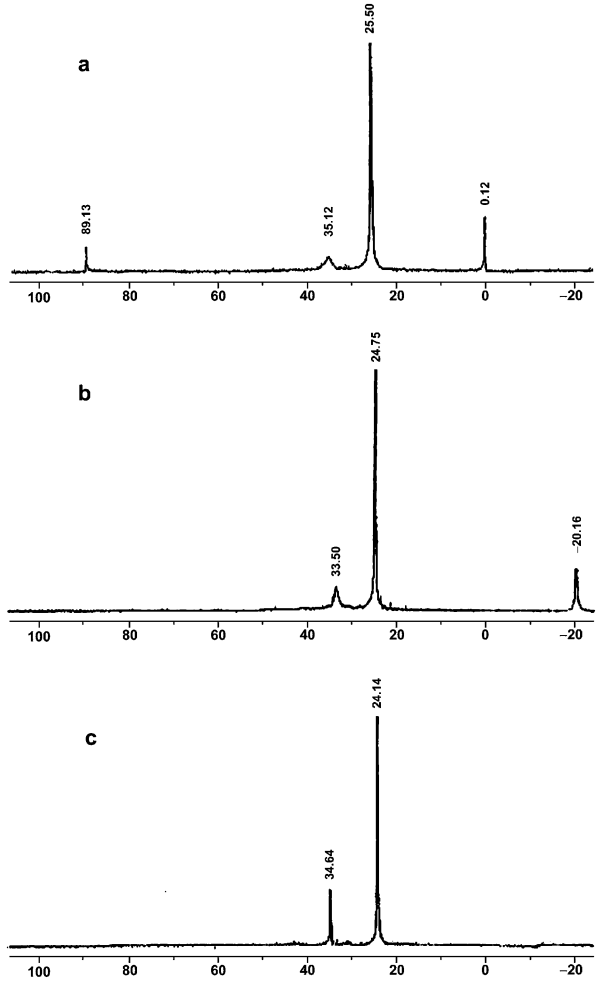

Figure 7. ^{31}P NMR spectra of the mixture of L1AuClO$_4$ and Ph_2PH in $CDCl_3$: (a) L1AuClO$_4$/Ph_2PH (1:5, molar ratio), −60 °C; (b) L1AuClO$_4$/Ph_2PH (1:20, molar ratio), −60 °C; (c) L1AuClO$_4$/Ph_2PH (1:20, molar ratio), −20 °C;

In view of the reversible interaction, the reaction dynamics between L1-metals and various phosphines were studied by fluorescence monitors. Dichloromethane solutions of L1Cu$^+$, L1Ag$^+$, and L1Au$^+$ (at 5×10^{-6} M) became strongly fluorescent on addition of tributylphosphine, diphenylphosphine, or triphenylphosphine ($\geq 10^{-5}$ M).[10a] When the solution of L1M$^+$ (5×10^{-6} M) was titrated with a solution of Ph_2PH (2.5×10^{-6} to 5×10^{-5} M), a significant enhancement of fluorescence was observed. As shown in Figure 8a, it reached the maximum at the ratio of 10 for L1Ag$^+$ and L1Au$^+$ and at that of 32 for L1Cu$^+$. The ratio demonstrated the dynamics of the coordinating interaction of PPh_2H, the equilibrium of which was in favor of L1-metals, particularly in the case of L1Cu$^+$. The *exocyclic* metal coordination of L1MP$^+$, as shown in Scheme 2, is proposed to visualize the reaction. The relative intensities compared with L1 (5×10^{-6} M) increase 3−5-fold, while compared with L1M$^+$ (5×10^{-6} M) they increase

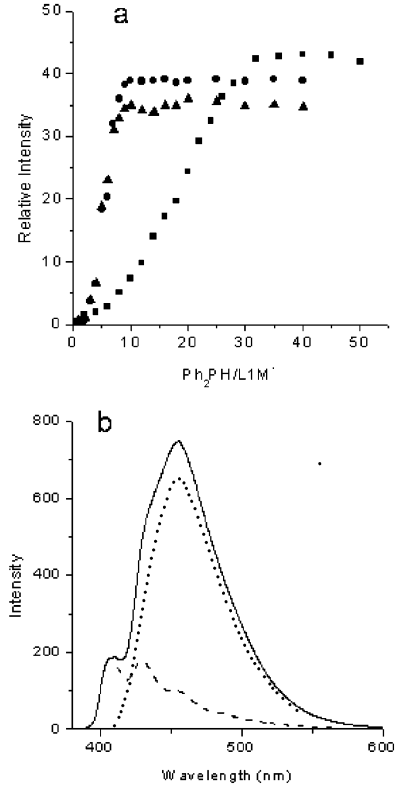

Figure 8. (a) Plots of recorded relative fluorescence intensities at 456 nm as in (b) against the ratio of $HPPh_2$/L1M$^+$; [L1M$^+$] = 5×10^{-6} M in dichloromethane (L1Cu$^+$, ■; L1Ag$^+$, ●; L1Au$^+$, ▲). (b) Fluorescence emission difference spectrum ($\lambda_{monitor}$ = 433 nm) between L1Ag$^+$ (5×10^{-6} M) in the presence of $HPPh_2$ (2×10^{-5} M) (—) and using 410 nm as the reference point and the emission curve of Figure 4c as a substitute for the L1AgP$^+$ fluorescence curve (- - -). (····) represents the fluorescence excimer spectrum.

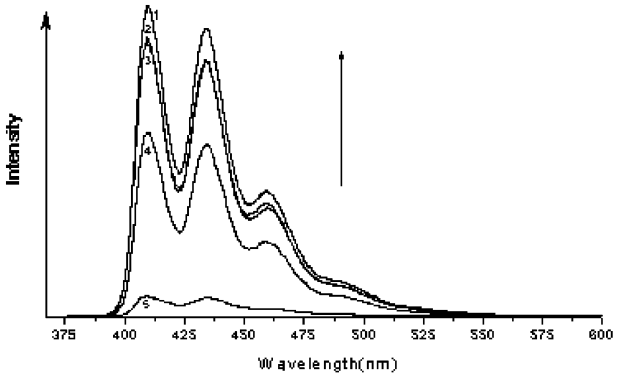

Figure 9. Fluorescence emission spectra of $L2Ag^+$ (1×10^{-5} M) in order of increasing PPh_2H at 5×10^{-5}, 1×10^{-4}, 2×10^{-4}, and 3×10^{-4} M in dichloromethane.

80−150-fold. Figure 8b shows the resolved curve of the fluorescence at $[L1Ag^+] = 5 \times 10^{-6}$ M in the presence of $HPPh_2$ at 2×10^{-5} M using 410 nm as the reference point and the emission curve of Figure 4c as a substitute for the $L1AgP^+$ fluorescence curve. This demonstrated that the new structureless band was broad and centered at about 456 nm.

Similarly, titration of Ph_2PH to a $L2Ag^+$ solution in CH_2Cl_2 (1×10^{-5} M) exhibits the sequential fluorescence enhancement, but the pattern demonstrated that the spectra were the anthracenoid type and no new peak appeared (Figure 9).

The interaction of L1-metals with Ph_2PH is represented by the coordination of metal to stabilize the *exocyclic* configuration in $L1M'^+$, which is present in low concentrations as in Figure 4c. Two consecutive unfavorable equilibria in Scheme 2 demand a high concentration of PPh_2H (e.g., $>1.5 \times 10^{-4}$ M for $L1Cu^+$) to complete the $L1MP^+$ formation. The first *endo*−*exo* equilibrium consists of the rupture of η^6 bonding to give unstable bis-coordinate $L1M'^+$. Thus, $L1M'^+$ is vastly unfavorable until coordinated by PR_3 (or chloride).

The presence of concentration-dependent new fluorescence at about 455 nm is ubiquitous in this series that includes L1, $L1MP^+$, and L1AuCl, but absent in $L2AgP^+$. The broad new emission must come from an excimer in each case, and the excimer interaction must involve a component of the L1 framework since $L2AgP^+$ does not show the excimer peak. Further, the excimer must have different geometry from that of the anthracene excimer having the π-orbital overlap since this and allied systems[13] fluoresce in the 570−580 nm region. Subject to future studies, we propose that the excited anthracene moiety of these substrates is modified by interaction with the N−P function of another substrate to give the new 456 nm fluorescence. The new 456 nm fluorescence has a broad shape typical for an excimer type, but a shorter lifetime ($\tau_1 = 2-3$ ns) than the parent anthracenoid fluorescence ($\tau_2 = 9-12$ ns). To our knowledge, an excimer from aromatic π-orbital interaction generally results in fluorescence at longer wavelengths and with longer lifetimes[14] that logically arise from stabilized complexes with a lower potential energy.[14d] The present excimer shows neither of these characteristics and may represent a transient type excimer which is derived from a modification of, rather than stabilization of, the parent excited state. It is a great challenge to delineate the conformation of such transient complexes in the future.

Fluorescence intensities of both L1 and L1AuCl were not affected by the presence of PR_3. Finally it should be added that the L1-metal fluorescence pattern was not affected at all in the presence of nitrogen ligands, such as acetonitrile, pyridine, and aniline. Therefore, the equilibrium pattern shown in Scheme 2 is a good reaction potentially adaptable for the off−on molecular switch design for phosphine in terms of selectivity and sensitivity.

Conclusions

Using a new fluoroionophore, two N−P coordinating groups containing L1, we have prepared novel nonemissive endocyclic group 11 metal aromatic η^6-complexes $L1M^+$. The three-center metal−NP and metal−η^6-arene bonding features in these complexes have been confirmed using ab initio and density functional calculations. Owing to the formation of the charge transfer complexes compound L1 functions as an on−off switch for these ions. The reversible interaction of $L1M^+$ with PR_3 maintains the *exocyclic* metal configuration, which affords strong fluorescence. Therefore, $L1M^+$ complexes function as off−on switches for the neutral molecule PR_3. The series of L1 compounds including L1, $L1MP^+$, and L1AuCl exhibits a new concentration-dependent emission at about 455 nm due to an excimer formation. We propose that the excited anthracene moiety of these substrates is modified by interaction with the N−P function of another substrate to give the new excimer.

Experimental Section

General Comments. All reactions were carried out under a nitrogen atmosphere using standard Schlenk or vacuum line techniques. All solvents were thoroughly dried and deoxygenated by standard methods and distilled immediately before use. Column chromatography was carried out using silica gel of 300−400 mesh. 9,10-Bis(*N*-propylaminomethyl)anthracene, L1, and $L1Ag^+$ were prepared according to literature methods.[7,10a] IR spectra were recorded on a Bruker FT-IR Equinox-55 infrared spectrophotometer in the range 4000−400 cm^{-1} using KBr disks. ^1H NMR and ^{31}P NMR spectra were recorded on a Bruker AC-200 NMR spectrometer. Elemental analyses were performed by a Yanaco MT-3 analyzer. The luminescent spectra and UV-absorption spectra were conducted on a Perkin-Elmer LS-50B luminescence spectrometer and a Shimadzu UV-1601PC UV−visible spectrophotometer, respectively. Melting points were determined on a Yanaco micromelting point apparatus MP-500. Luminescence decay measurements of the ligand and complexes were performed with a Horiba NAES-1100 single photon counting nanosecond fluorescence spectrometer.

Preparation of L1Cu Perchlorate. To a solution of anthracenodiphosphine L1 (0.344 g, 0.50 mmol) in CH_2Cl_2 (20 mL) was added solid $Cu(CH_3CN)_4ClO_4$ (0.164 g, 0.5 mmol) under dinitrogen, and the resulting solution was stirred for 2 h at room temperature. The filtrate, after filtering off some

(13) (a) Sclafani, J. A.; Maranto, M. T.; Sisku, T. M.; Arman, S. A. V. *Tetrahedron Lett.* **1996**, *37*, 2193. (b) Tahara, R.; Hasebe, K.; Nakamura, H. *Chem. Lett.* **1995**, 953.

(14) (a) Forster, T.; Kasper, K. *Z. Physik. Chem. N. F.* **1954**, *1*, 275. (b) Yoshihara, K.; Kasuya, T.; Inoue, A.; Nagakura, S. *Chem. Phys. Lett.* **1971**, *9*, 469. (c) Chow, Y. L.; Cheng, X. E.; Johansson, C. I. *J. Photochem. Photobiol. A: Chem.* **1991**, *57*, 247. (d) Chow, Y. L.; Johansson, C. I. *Chem. Phys. Lett.* **1994**, *231*, 541. (e) Chow, Y. L.; Johansson, C. I. *J. Phys. Chem.* **1995**, *99*, 17558.

insoluble materials, was diluted with diethyl ether to afford air-stable yellow crystals of L1Cu perchlorate (0.240 g, 75.3%), mp 220−222 °C. Anal. Calcd for $C_{46}H_{46}ClCuN_2O_4P_2$: C, 64.98; H, 5.70; N, 3.06. Found: C, 64.83; H, 5.40; N, 3.06. ^{1}H NMR ($CDCl_3$): 0.67−0.83 (t, J = 7 Hz, 6H, $2CH_3$), 1.40−1.75 (m, 4H, $2CH_2$), 3.06−3.20 (t, J = 7 Hz, 4H, $2CH_2$), 5.20−5.30 (s, 4H, $2CH_2$), 6.64−6.84 (m, 8H, C_6H_5), 7.10−7.24 (m, 8H, C_6H_5), 7.46−7.60 (m, 4H, C_6H_5), 7.70−7.81 (m, 4H, 4CH), 8.32−8.45 (m, 4H, 4CH) ppm. ^{31}P NMR ($CDCl_3$): 34.56 (s) ppm.

Preparation of L1AuCl. To a solution of anthracenodiphosphine L1 (0.171 g, 0.25 mmol) in CH_2Cl_2 (15 mL) was added solid $Au(SMe_2)Cl$ (0.074, 0.25 mmol), and the resulting solution was stirred for 3 h at room temperature. The filtrate, after filtering off some insoluble materials, was diluted with diethyl ether to afford air-stable yellow crystals of L1AuCl (0.211 g, 91.6%), mp 220−222 °C. Anal. Calcd for $C_{46}H_{46}ClN_2P_2Au\cdot1.5CH_2Cl_2$: C, 54.41; H, 4.71; N, 2.67. Found: C, 55.09; H, 4.20; N, 2.54. ^{31}P NMR ($CDCl_3$): 75.53 (s) ppm.

Preparation of L1Au Perchlorate. To a solution of anthracenodiphosphine L1 (0.172 g, 0.25 mmol) in CH_2Cl_2 (15 mL) was added solid $Au(SMe_2)Cl$ (0.074, 0.25 mmol), and the resulting solution was stirred for 3 h at room temperature. Then solid $AgClO_4$ (0.054 g, 0.25 mmol) was added, the resulting mixture was stirred for 0.5 h at room temperature, and the mixture was centrifugally separated to remove generated AgCl. Diethyl ether was diffused into the concentrated solution to give L1Au perchlorate (0.212 g, 86.2%) as a yellow crystal, mp 256−258 °C. Anal. Calcd for $C_{46}H_{46}AuClN_2O_4P_2$: C, 56.08; H, 4.71; N, 2.84. Found: C, 55.92; H, 4.61; N, 3.10. ^{31}P NMR ($CDCl_3$): 70.60 (s) ppm.

Preparation of L2. A solution of *n*-BuLi in hexane (2.18 M, 21.1 mL) was added dropwise to a solution of Ph_2PH (7.6 mL, 44 mmol) in 200 mL of tetrahydrofuran at 0 °C. The resulting mixture was added dropwise to a solution of 9,10-bis(2-chloroethyl)anthracene (6.06 g, 20 mmol) in 50 mL of tetrahydrofuran at 0 °C, after which the mixture was stirred for 4 h at room temperature. The solvent was removed in a vacuum, and water (200 mL) was added. The aqueous phase was extracted with CH_2Cl_2 (3 × 300 mL) and the organic phase dried with anhydrous $MgSO_4$ overnight. Most of the CH_2Cl_2 was removed in a vacuum, and diethyl ether was added to deposit a colorless solid, which upon recrystallization from CH_2Cl_2/diethyl ether afforded an analytically pure product, L2, 4.9 g (40.8%), mp 236−238 °C. Anal. Calcd for $C_{42}H_{36}P_2\cdot CH_2Cl_2$: C, 75.11; H, 5.57. Found: C, 74.73; H, 5.61. ^{1}H NMR (d_6-DMSO): 3.94−3.97 (t, 4H, $2CH_2$); 4.07−4.10 (t, 4H, $2CH_2$), 7.54−7.63 (m, 20H, $4C_6H_5$), 7.90−8.10 (m, 4H, 4CH), 8.35−8.41 (m, 4H, 4CH). ^{31}P NMR: −12.9 ppm.

Preparation of L2Ag Perchlorate. To a solution of L2 (0.24 g, 0.40 mmol) in CH_2Cl_2 (20 mL) was added solid $AgClO_4$ (0.083 g, 0.40 mmol), and the mixture was stirred for 4 h at room temperature. The filtrate of the mixture was evaporated to a small volume. The residue was diluted with ether to give yellow crystals of L2Ag perchlorate (0.24 g, 74.1%), mp 210−212 °C. Anal. Calcd for $C_{42}H_{36}AgClO_4P_2$: C, 62.28; H, 4.48. Found: C, 62.16; H, 4.50. ^{31}P NMR ($CDCl_3$): 0.08 ($J_{P-107Ag}$ = 508.9 Hz; $J_{P-109Ag}$ = 581.3 Hz) ppm.

X-ray Diffractions of Single-Crystal Structural Determination. Diffraction experiments were performed on a Bruker Smart 1000 CCD diffractometer employing graphite-monochromatized Mo Kα radiation (λ = 0.71073 Å) and collecting a hemisphere of data in 1329 frames with 10 s exposure times. The atom positions were determined using direct methods employing SHELXTL-97 and successive difference Fourier map calculations. The full-matrix least-squares refinement was carried out on F^2. All non-hydrogen atoms were assigned anisotropic temperature factors. Empirical absorption corrections were applied to the data sets employing SADABS. Most hydrogen atom positions were calculated and allowed to ride on the carbon to which they are bonded assuming a C−H bond length of 0.95 Å. Hydrogen atom temperature factors were fixed at 1.20 times the isotropic temperature factor of the carbon atom to which they are bonded. The hydrogen atom contributions were calculated, but not refined.

X-ray Crystallography. Crystallography data (excluding structure factors) for the structures reported in this paper have been deposited with the Cambridge Crystallographic Data Centre as supplementary publication nos. CCDC-188735 ($L1AgClO_4$), CCDC-188736 ($L1CuClO_4$), CCDC-188737 ($L1AuClO_4$), and CCDC-188738 ($L2AgClO_4\cdot0.5CH_2Cl_2$). Copies of the data can be obtained free of charge on application to CCDC, 12 Union Road, Cambridge CB2 1EZ (UK) (fax: (+44) 1223-336-033; e-mail: deposit@ccdc.cam.ac.uk).

Theoretical Calculations. All theoretical calculations were performed on a PC using Gaussian 98.[11a] All electron basis sets STO-3G* and 3-21G*[11b,c] for Cu and Ag complexes and the ECP set LanL2DZ[11d] for all including $L1Au^+$ were used. The geometries were taken from their X-ray crystallographic data.

Acknowledgment. We gratefully acknowledge the financial assistance provided by the National Natural Science Foundation of China (Project No. 20102003).

Supporting Information Available: Full tables of atomic coordinates, thermal parameters, and a full list of bond lengths and bond angles for complexes $L1Cu^+$, $L1Au^+$, and $L2Ag^+$. This material is available free of charge via the Internet at http://pubs.acs.org.

OM020668H